Development/Plasticity/Repair

α4* Nicotinic Acetylcholine Receptors Modulate Experience-Based Cortical Depression in the Adult Mouse Somatosensory Cortex

Craig E. Brown,[1,2,3] Danielle Sweetnam,[1] Maddie Beange,[1] Patrick C. Nahirney,[1,2] and Raad Nashmi[2]

[1]Division of Medical Sciences and [2]Department of Biology, University of Victoria, Victoria, British Columbia V8P 5C2, Canada, and [3]Department of Psychiatry, University of British Columbia, Vancouver, British Columbia V6T 2A1, Canada

The molecular mechanisms that mediate experience-based changes in the function of the cerebral cortex, particularly in the adult animal, are poorly understood. Here we show using *in vivo* voltage-sensitive dye imaging, that whisker trimming leads to depression of whisker-evoked sensory responses in primary, secondary and associative somatosensory cortical regions. Given the importance of cholinergic neurotransmission in cognitive and sensory functions, we examined whether α4-containing (α4*) nicotinic acetylcholine receptors (nAChRs) mediate cortical depression. Using knock-in mice that express YFP-tagged α4 nAChRs subunits, we show that whisker trimming selectively increased the number α4*-YFP nAChRs in layer 4 of deprived barrel columns within 24 h, which persisted until whiskers regrew. Confocal and electron microscopy revealed that these receptors were preferentially increased on the cell bodies of GABAergic neurons. To directly link these receptors with functional cortical depression, we show that depression could be induced in normal mice by topical application or micro-injection of α4* nAChR agonist in the somatosensory cortex. Furthermore, cortical depression could be blocked after whisker trimming with chronic infusions of an α4* nAChR antagonist. Collectively, these results uncover a new role for α4* nAChRs in regulating rapid changes in the functional responsiveness of the adult somatosensory cortex.

Introduction

Sensory deprivation is known to trigger a long-lasting depression of neuronal responsiveness in primary visual and somatosensory cortices (Wiesel and Hubel, 1963; Buonomano and Merzenich, 1998; Wright et al., 2008). Although it is certain that cortical depression takes place, the molecular mechanisms that mediate this form of plasticity are not well understood, especially for adult animals that are less well studied. Thus far, mechanistic studies conducted primarily in young animals have implicated glutamate (Rema et al., 1998; Takahashi et al., 2003; Clem et al., 2008; Wright et al., 2008; Dachtler et al., 2011) and cannabinoid (L. Li et al., 2009) receptor signaling in experience-based cortical depression. This leaves open the possibility that other modulators of synaptic signaling, perhaps acting through inhibitory circuits which have recently been implicated in visual (Yazaki-Sugiyama et al., 2009) and barrel cortex plasticity (Jiao et al., 2006; Sun, 2009) may be involved.

Cholinergic neurotransmission has long been implicated in cortical plasticity (Kilgard and Merzenich, 1998). For example, lesions of the basal forebrain cholinergic system cause impairments in motor learning and cortical map plasticity associated with stroke or peripheral nerve transection (Juliano et al., 1991; Conner et al., 2003; Conner et al., 2005). Although these studies have indicated cholinergic involvement in cortical plasticity, it was not clear which specific cholinergic receptor was involved. Thus far, much attention has focused on the functional significance of muscarinic receptors in cortical plasticity (Maalouf et al., 1998; Shulz et al., 2000). However, it seems plausible that nicotinic acetylcholine receptors (nAChRs) may also play an important role in experience-based cortical plasticity. Neuronal nAChRs are ligand-gated, cation-permeable channels that are assembled in pentamers composed in a variety of subunit combinations (α2-α10 and β2-β4; (Dani, 2001; Barik and Wonnacott, 2009), with the α4* bearing nAChR being the most prevalent (* indicates that there are other subunits in the pentameric nAChR). Studies have shown that nAChRs can regulate synaptic plasticity in the hippocampus and reward pathways (McKay et al., 2007; Nashmi et al., 2007; Changeux, 2010). In the visual cortex, these receptors are highly expressed during the critical period of ocular dominance plasticity (Prusky et al., 1988), which can be extended by removing a molecular brake on nAChR function (Morishita et al., 2010). Furthermore, nAChRs are expressed on GABAergic neurons throughout the cerebral cortex which can directly control the excitability and plasticity of corti-

Received Sept. 7, 2011; revised Nov. 18, 2011; accepted Dec. 8, 2011.

Author contributions: C.E.B. designed research; C.E.B., D.S., M.B., and P.C.N. performed research; R.N. contributed unpublished reagents/analytic tools; C.E.B., D.S., M.B., and P.C.N. analyzed data; C.E.B. wrote the paper.

This work was supported by grants to C.E.B. from the Natural Sciences and Engineering Research Council (NSERC), the Canadian Institutes of Health Research, and the Heart and Stroke Foundation. R.N. was supported by NSERC discovery and equipment grants, a National Alliance for Research on Schizophrenia and Depression Young Investigator Award, the Myre and Winifred Sim Fund, and the Canada Foundation for Innovation. We thank Thomas Watson and Isaiah Geise for collecting preliminary data. We also thank Dr. Leigh Ann Swayne and Andrew Holmes for their comments on the manuscript.

Correspondence should be addressed to Dr. Craig E. Brown, Assistant Professor, Division of Medical Sciences and Department of Biology, Medical Sciences Building, PO Box 1700 STN CSC, University of Victoria, Victoria, BC V8W 2Y2, Canada. E-mail: brownc@uvic.ca.

DOI:10.1523/JNEUROSCI.4568-11.2012

 0270-6474/12/321207-13$15.00/0

cal pyramidal neurons (Xiang et al., 1998; Porter et al., 1999; Disney et al., 2007). Given these functional and anatomical studies, it is conceivable that nAChRs could regulate cortical depression in the adult somatosensory cortex.

Here, we used the whisker-to-barrel cortex pathway to examine the role of nAChRs in experience-based depression of the adult somatosensory cortex. Using a battery of imaging approaches such as *in vivo* voltage-sensitive dye (VSD) imaging, confocal and electron microscopy, we provide new evidence that implicates $\alpha4^*$ nAChRs in the regulation of experience-based cortical depression.

Materials and Methods

Animals and whisker trimming. Adult (2.5–4 months old) male wild-type or $\alpha4$-YFP knock-in mice (Nashmi et al., 2007) with C57BL/6J background were used. The $\alpha4$-YFP knock-in mice also co-expressed a hemagglutinin (HA) epitope tag. All experiments were conducted in accordance with the guidelines set by the Canadian Council for Animal Care. Mice were group housed in clear plastic cages under a 12 h light/dark cycle and given *ad libitum* access to food and water. For trimming, mice were lightly anesthetized with 1.5% isoflurane gas mixed with oxygen and had whiskers cut unilaterally to a height of 3–5 mm from the face. After trimming, mice were returned to their home cage. In some rare instances, we excluded mice from the study that been barbered by their cage mates.

VSD imaging. On the day of imaging, mice were anesthetized with an initial injection of 15% urethane (w/v) dissolved in distilled water (1.25 g/kg). To maintain a sufficient depth of anesthesia, mice would receive supplementary injections of urethane every 1–2 h (0.125 mg/kg). Body temperature was carefully regulated throughout the experiment and kept at 37°C with a rectal thermoprobe and temperature feedback regulator. Adequate hydration was maintained by injecting 0.2 ml of 20 mM glucose (i.p.) every 1–2 h. Physiologic parameters including heart rate, respiration and blood oxygen saturation were monitored in a subset of animals using a mouse pulse oximeter (Starr Life Sciences Corp.) mounted on the right hindlimb. To perform the craniotomy, we used a high speed dental drill to thin the skull outlining a 5 × 7 mm region over the right cerebral hemisphere. For very lateral aspects of the craniotomy, we carefully teased back a portion of the temporalis muscle. Buffer was applied to the skull intermittently to keep the skull moist and the brain cool from drilling. Fine-tipped surgical forceps were used to remove the piece of skull and the dura. Gel foam soaked in HEPES-buffered artificial CSF (aCSF) was used to keep the brain moist throughout the surgical procedure. The brain was stained with the voltage-sensitive dye RH1692 dissolved in HEPES-buffered aCSF (Optical Imaging, 1 mg/ml passed through 0.22 μm syringe filter) for 60–75 min. After dye incubation, the brain was washed thoroughly, covered with 1.3% low-melt agarose dissolved in aCSF and sealed with a custom cut glass coverslip. Movement artifacts during imaging were further minimized by cementing a small plate to the skull of the mouse which was then fastened to metal posts that would hold the mouse steady under the microscope.

For pharmacological experiments, the craniotomy was performed as described above with the exception that low-melt agarose was applied only to the edges of the craniotomy to keep the brain still, with a coverslip floating on top of aCSF. Whisker-evoked cortical responses were imaged for at least 15 min to obtain a stable baseline measurement before topical application or micro-injection of 0.5 or 1 mM the $\alpha4^*$ nAChR agonist RJR-2403 (Tocris Bioscience; dissolved in aCSF). To directly modulate $\alpha4^*$ nAChRs in layer 4, glass micropipettes with a 5 μm tip were filled with 0.5 mM RJR-2403 or antagonist dihydro-β-erythroidine hydrobromide (DHβE, Tocris Bioscience) dissolved in aCSF. Pipettes were slowly inserted into the cortex at a 30° angle to a depth of ~450 μm to reach layer 4. Drugs were pressure ejected and the injection site was marked with 1% Texas Red dextran (70 kDa, Invitrogen) and verified by postmortem histology.

For VSD imaging, 12-bit image frames (184 × 124 pixels) were captured every 4 ms using a MiCAM02 camera (Brain Vision). The dye was excited with Luxeon K2 red LED (627 nm, ~20 mW at back aperture) that was passed through a Cy5 filter cube (exciter: 605–650 nm, emitter: 670–720 nm) in an Olympus BX51WI upright microscope. Red light was focused 200–300 μm below the cortical surface using an Olympus XFluor 2× objective [numerical aperture (NA) = 0.14]. During each trial, images were collected 250 ms before a single 1 ms deflection of the whisker (or not for null stimulation trials) and then 550 ms afterward. Whisker stimulation was achieved by a computer controlled trigger of a piezoelectric wafer (Q220-AY-203YB, Piezo Systems) that deflected the whisker ~300 μm in the caudal-rostral plane. This process was repeated 15–30 times for each whisker, with a 10 s interval between trials. To correct for dye bleaching, stimulation trials were divided by null stimulation trials. VSD images were presented as the percentage change in VSD fluorescence ($\Delta F/F_o$) by dividing frames collected after stimulation by the average of those taken 100 ms before stimulation. Montages of cortical responses shown in the figures were generated by summing up all trials for each whisker, then mean filtering $\Delta F/F_o$ image stacks (radius = 2) and binning 2 frames in time (hence 8 ms between each image).

The peak amplitude and latency of cortical responses to whisker deflection were quantified from raw unfiltered images using a circular region of interest (370 μm in diameter; Fig. 1*D*) placed over the primary somatosensory (S1), secondary somatosensory (S2), or parietal association (PA) cortex where cortical responses first emerged in each site. Data were exported to Clampfit 9.0 software (Molecular Devices) which provided the peak amplitudes, time to peak amplitude and half-width (i.e., duration) of VSD signals in the first 250 ms after stimulation.

Anterograde tracing of thalamic axons. Mice were anesthetized with 1.5% isoflurane and placed into a stereotaxic frame. A small hole was drilled 1.8 mm posterior and 1.4 mm lateral of bregma. Thalamic axons from the ventral posterior medial nucleus were labeled by lowering a Hamilton syringe 3.5 mm deep into the brain and slowly releasing 0.2 μl of 5% Mini-ruby (dissolved in aCSF, molecular weight = 10,000, Invitrogen) over 5 min. Mice survived for 5 d and were then perfused with 5 ml 0.1 M PBS, pH 7.4, followed by 5 ml of 4% paraformaldehyde (PFA) in PBS.

Immunohistochemistry. Mice were overdosed with sodium pentobarbital anesthetic and transcardially perfused with 5 ml of PBS followed by 10 ml of 4% PFA in PBS. Whole brains or flattened cerebral hemispheres (for tangential sectioning to visualize the barrel field in layer 4) were postfixed in 4% PFA for 3–5 h and then transferred to PBS or 30% sucrose solution. Brain sections were cut at 40 μm on a vibratome in the coronal or tangential plane. For immunofluorescence experiments, sections from $\alpha4$-YFP mice were incubated overnight at room temperature in PBS containing a single primary antibody for mouse anti-NeuN (1:200, Millipore Bioscience Research Reagents), rabbit anti-GABA (1:1000, Sigma), rabbit anti-vesicular GABA transporter (VGAT, 1:500, Millipore), guinea pig anti-VGlut1 or 2 (1:500, Millipore), rabbit anti-vesicular acetylcholine transporter (VAChT, 1:250, Abcam), goat anti-choline acetyltransferase (ChAT, Millipore) or rabbit anti-PSD-95 (postsynaptic density protein; 1:400, Invitrogen). Sections were washed in PBS and then incubated for 4 h at room temperature with Cy5-conjugated secondary antibodies (1:400, Jackson Immunoresearch Laboratories). After incubation, sections were washed in PBS, mounted onto glass slides and coverslipped with fluorescent mounting media (Fluoromount-G, Southern Biotech).

Sections were imaged with a 60× oil objective (NA = 1.35) using an Olympus confocal microscope controlled by Fluoview software. High resolution image stacks were collected sequentially using 515 and 635 nm lasers to excite YFP and Cy5 fluorophores, respectively. Image stacks were collected in 0.5 μm *z*-steps at 12 bit intensity resolution at 1024 × 1024 pixels (0.065 μm/pixel) with a pixel dwell time of 8 μs. Sections in which the primary antibody was omitted served as controls for imaging. To quantify changes in the number of $\alpha4$-YFP puncta or ChAT expression after trimming, 40 images, each with an area of 4430.2 μm^2 were analyzed. Therefore the total volume of tissue that puncta were quantified from was typically 88,604 μm^3. To remove background fluorescence, a duplicate of each image projection was smoothed (mean filter of 80) and subtracted from the original image. The number and size of $\alpha4$-YFP or ChAT puncta in each barrel were quantified using a particle analysis macro in NIH ImageJ (version 1.44d). Automated counts were

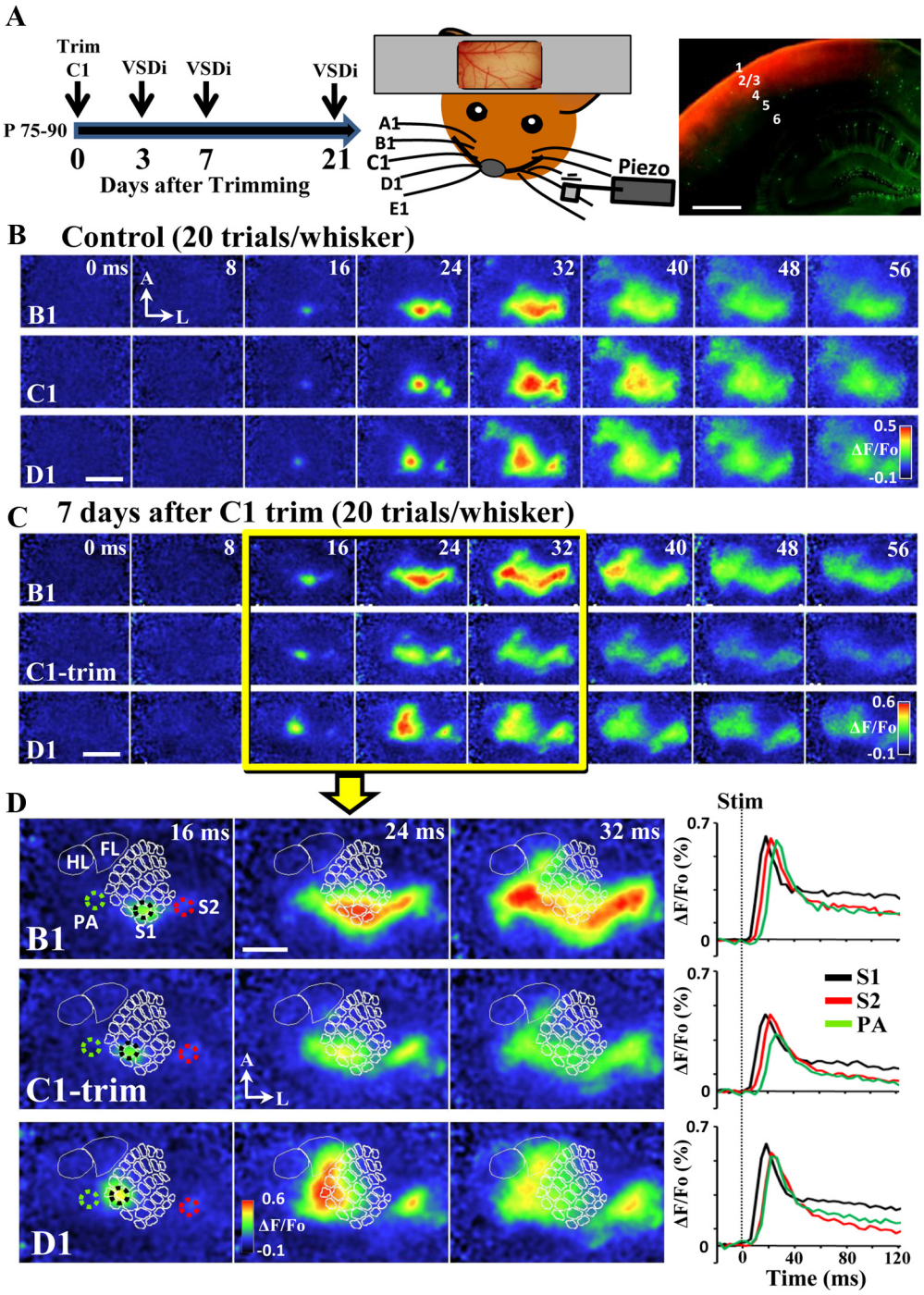

Figure 1. VSD imaging reveals depressed sensory-evoked responses in somatosensory cortex after whisker trimming. ***A***, Summary of imaging experiments used to determine the time course of cortical depression after trimming. Fully mature mice were prepared for *in vivo* VSD imaging 3, 7, or 21 d after trimming the left C1 whisker (left). Note that VSD imaging is done at singular time points and not performed repeatedly in the same animal. Single whiskers were deflected with a 1 ms flick from a pencil lead connected to a piezo-electric wafer (middle). Coronal sections revealed that VSD 1692 penetrated superficial layers 1–4 (right). Scale bar, 1 mm. ***B***, Montages showing the spatiotemporal dynamics of cortical responses to deflection of either the B1, C1, or D1 whisker (indicated as time 0 ms) in a sham trimmed control mouse. Scale bar, 2 mm. ***C***, Seven days after trimming the C1 whisker, cortical responses to the trimmed whisker are reduced relative to nondeprived whiskers B1 and D1. Scale bar, 2 mm. ***D***, Montage showing sequential activation of whisker-evoked responses in S1, S2, and PA cortex in a trimmed mouse. Cortical depolarizations first appeared in S1 cortex followed by S2 cortex and then PA cortex. Note that trimming lowers the amplitude of C1-evoked responses, but does not alter the timing or general pattern of cortical activation in S1, S2, and PA cortex. Graphs on the right-hand side plot the percentage change in fluorescence relative to baseline (% $\Delta F/F_0$) in each cortical region where responses first emerged (see placement of dashed circles). Plots were generated from an average of 15 stimulation trials per whisker. Scale bar, 1 mm.

validated by comparing these values to those obtained from blind manual counting of puncta. For determining α4-YFP colocalization with markers of presynaptic or postsynaptic sites (e.g., PSD-95), images in each channel were manually thresholded and then overlaid. Puncta that overlapped 10 pixels or more (~20% overlap given the average size of YFP puncta) were considered to be colocalized.

Electron microscopy. Immunostaining for HA on YFP-tagged α4* nAChRs (Nashmi et al., 2007) was achieved by immersing fixed brain sections in 0.3% H_2O_2 for 15 min followed by overnight incubation in PBS containing rabbit anti-HA antibodies (1:1000, Sigma). Sections were then incubated for 2 h in PBS containing biotin-conjugated anti-rabbit antibodies (1:1000, Vectastain Elite kit, Vector Labs), followed by incu-

Table 1. Quantification of the time to peak and duration of C1-evoked responses in S1, S2, and PA cortex

Cortical responses to C1 whisker stimulation	Control	3 d	7 d	21 d	ANOVA, *p* value
S1					
Time to peak response (ms)	22.6 ± 1.3	28.4 ± 3.1	28.0 ± 2.9	19.9 ± 1.0	$F_{(3,25)} = 2.71, p = 0.06$
Duration of response (ms)	45.8 ± 10.0	52.9 ± 5.5	61.5 ± 15.9	41.3 ± 9.7	$F_{(3,25)} = 0.50, p = 0.68$
S2					
Time to peak response (ms)	27.8 ± 0.66	30.4 ± 2.4	27.4 ± 1.7	23.1 ± 2.0	$F_{(3,25)} = 2.67, p = 0.07$
Duration of response (ms)	28.3 ± 2.4	39.9 ± 5.1	44.5 ± 8.5	28.1 ± 3.2	$F_{(3,25)} = 2.55, p = 0.08$
PA					
Time to peak response (ms)	30.0 ± 1.6	42.4 ± 4.3	39.1 ± 5.2	28.6 ± 1.0	$F_{(3,21)} = 2.54, p = 0.08$
Duration of response (ms)	29.5 ± 2.7	28.8 ± 5.3	53.6 ± 13.2	34.2 ± 9.1	$F_{(3,21)} = 1.80, p = 0.17$

Values are mean ± SEM.

bation in streptavidin-HRP (1:1000, Vector Labs) for 1 h. HA was visualized by reacting sections with chromagen solution (0.2 mg/ml diaminobenzidine, 0.01% H_2O_2, and 0.4 mg/ml nickel chloride) for 10–15 min. Sections were then fixed in 2% glutaraldehyde and 2% paraformaldehyde in 0.1 M Na-cacodylate buffer, pH 7.4, for 1 h at room temperature. Sections were washed in cacodylate buffer and layer 4 of the primary somatosensory cortex was dissected out and cut into 1 × 1 mm pieces. Samples were then lightly postfixed with 1% osmium tetroxide in cacodylate buffer (15 min at room temperature), washed with dH_2O and dehydrated with ascending ethanols to 100%. Tissue blocks were infiltrated with Spurr's low viscosity embedding resin overnight, embedded in capsules, and polymerized overnight at 65°C. Tissue blocks were sectioned at 70 nm thickness with a diamond knife on an ultramicrotome, collected on 200 mesh copper grids and observed on a JEOL 1400 transmission electron microscope equipped with a Gatan SC1000 digital camera.

Cortical field potential recording. To determine how long nAChR antagonist DHβE affects whisker-evoked cortical responses, mice were anesthetized with urethane and had a Teflon-coated stainless steel wire (0.2 mm diameter) inserted into the C1 whisker representation that was determined using intrinsic signal optical imaging (Brown et al., 2009). A reference electrode was placed in the contralateral forelimb cortex. Whisker-evoked potentials (WEPs) were amplified (×1000) and filtered between 1 and 1000 Hz using a differential amplifier (A-M Systems, model 1700) and digitized at 10 kHz. WEPs were recorded every 10 s and averaged over 10 min epochs for 20 min before subcutaneous injection of DHβE (1 mg/kg) and 120 min afterward. Similar to previous work (Benison et al., 2006), field potentials consisted of a sharp biphasic waveform with a prominent "P1 and N1" component. Using Clampfit software, we measured the effect of DHβE on the peak amplitude between P1 and N1 components and expressed these values as the percentage change from preinjection/baseline amplitudes.

Mini-pump implantation. To chronically block α4* nAChR *in vivo* after whisker trimming, mice were subcutaneously implanted with a mini-pump (Alzet, model 1003D) filled with 0.9% saline (control) or DHβE. DHβE was infused over 3 d at a dose of 1 $mg \cdot kg\ h^{-1}$, using a flow rate of 1 μl/h. Previous data has shown that DHβE is nontoxic and metabolized rapidly. Three days after trimming and implantation, mini-pumps were removed ~5 h before the start of VSD imaging (except for 1 mouse ~3.5 h) or before they were killed for histological analysis of α4YFP puncta.

Statistical analysis. One-way ANOVA and Student's *t* tests with Bonferroni corrections were used to analyze data for main effects and statistical significance. All data are expressed as mean ± SEM.

Results

VSD imaging reveals depressed cortical responses after whisker trimming

VSD imaging is a useful tool for studying experience-dependent cortical plasticity because it allows one to visualize sensory cortical depolarizations with millisecond time resolution across a large region of cortex (Grinvald and Hildesheim, 2004). Further, VSD signals primarily reflect neuronal depolarizations from superficial cortical layers (Petersen et al., 2003) which remain plastic well into adulthood. To our knowledge, no previous study has used this approach to document cortical depression that occurs after whisker trimming, although a recent study proved that VSD imaging could detect functional changes in cortical representations after whisker pairing (Wallace and Sakmann, 2008). Therefore our first goal was to characterize the nature and time course of experience-based cortical depression using our imaging approach. For our initial set of experiments, we trimmed the C1 whisker on the left side of the face (only once) in 2.5–4-month-old mice (Fig. 1*A*). Only the C1 whisker was trimmed because previous work has shown that single whisker trimming induces maximal cortical depression (Wallace and Fox, 1999). Control mice were handled and in some cases lightly anesthetized with 1.5% isoflurane for the same period of time as trimmed mice. Three, 7, or 21 d after trimming, mice were anesthetized with urethane and had a 7 × 5 mm piece of the skull and dura removed over the right cerebral hemisphere (Brown et al., 2009). After incubation in 1 mM VSD (RH-1692, Optical Imaging), which stains superficial cortical layers, cortical responses were imaged following a 1 ms deflection of a single whisker (Fig. 1*A*). To stimulate cut whiskers in the 3 d group at the same distance from the face as other groups, we removed the C1 whisker on the right side of the face and then glued that to the stump of the trimmed C1 whisker on the left side. Control experiments indicated that this had no effect on the amplitude of C1 whisker-evoked cortical responses (peak $\Delta F/F_o$ in S1 for intact whisker = 0.22 ± 0.01% vs reattached whisker = 0.22 ± 0.02%). Therefore, any depression of cortical responses could not be attributed to simply stimulating a cut whisker.

In both control mice (Fig. 1*B*) and mice that had been trimmed (Fig. 1*C*), whisker stimulation induced a robust depolarization in the S1 cortex that was first evident within 16 ms (Fig. 1*B*,*C*), peaked ~22–28 ms after stimulation (Fig. 1*B*,*C*; Table 1), and then progressively dissipated within 100 ms of stimulus onset. In agreement with multielectrode field recordings (Brett-Green et al., 2004; Frostig et al., 2008) and VSD imaging of whisker-evoked cortical responses (Ferezou et al., 2006, 2007), subsequent depolarizations were observed lateral to the barrel field in the secondary somatosensory (S2) cortex and then directly medial to the barrel-field in the PA cortex (Fig. 1*D*). This pattern of cortical activation was observed following whisker stimulation in all but three mice (25 of 28 mice) where we could not detect a clear response in the PA cortex (Fig. 2*C* relative to Fig. 2*A*, this is reflected in the slightly reduced sample size). To quantify cortical responses, we plotted the change in fluorescence relative to baseline in each of the three cortical areas (Fig. 1*D*, see $\Delta F/F_o$ plots). Responses for each cortical region were measured where depolarizations first emerged (Fig. 1*D*, see placement of dashed circles). Note that whisker stimulation evoked spatially distinct responses in S1 cortex that were in direct register with anatomical

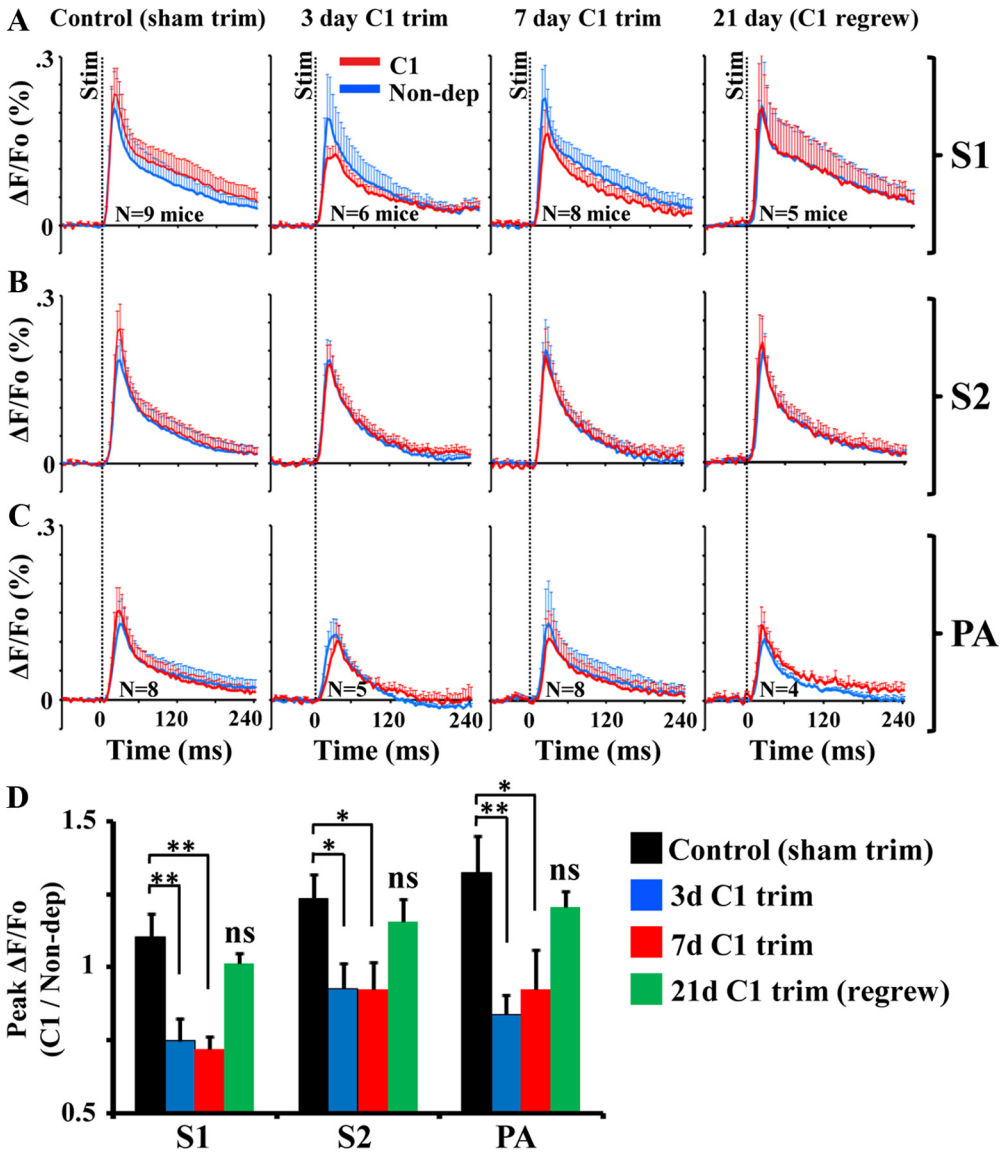

Figure 2. Quantitative changes in whisker-evoked cortical responses after trimming. ***A–C***, Each of the 12 plots shown represents the group average cortical response (measured as percentage $\Delta F/F_o$) to stimulation of the C1 whisker (red trace) or adjacent nondeprived whiskers (blue trace) for each time point and brain region. Note that the peak amplitude of C1-evoked responses (red trace) drops at 3 and 7 d after trimming in all three cortical areas relative to C1 whisker stimulation in control mice (without trimming) or to responses generated from stimulating adjacent nondeprived whiskers (see blue traces). Average cortical responses to nondeprived whisker stimulation (blue traces) changed very little after trimming. ***D***, Histogram showing normalized peak amplitude of cortical responses to C1 whisker stimulation (numerator) relative to nondeprived whiskers (denominator). Cortical responses to the trimmed whisker were significantly depressed 3 and 7 d after trimming, but not at 21 d when the whisker had regrown. Error bars represent SEM. $^*p < 0.05$, $^{**}p < 0.01$.

"barrels," whereas cortical responses to different whiskers showed considerable overlap in the S2 and PA cortices (Fig. 1*D*). Cortical responses peaked in S1 cortex first (black line), followed by S2 (red line) and then PA cortex (green line). Evidence of cortical depression can also be observed in these plots, given that the peak amplitude of C1-trimmed whisker responses were appreciably lower in S1, S2, and PA cortices than what was found after stimulation of nondeprived whiskers B1 or D1 (Fig. 1*D*).

To summarize whisker-evoked cortical responses across all experiments, we plotted $\Delta F/F_o$ (%) values in all three cortical regions in each mouse, and then generated an average trace for C1 (red trace) and nondeprived (blue trace) whisker responses for each group (Fig. 2*A–C*). As shown in Figure 2*A–C*, average C1 whisker responses in control mice were slightly higher than the average of nondeprived whisker responses in all three cortical regions. However, 3 and 7 d after C1 trimming, the peak amplitude of C1 whisker responses decreased considerably in these cortical regions (~25–50% reduction), whereas nondeprived whisker responses were relatively unchanged (note that in Fig. 2*A–C*, the red trace drops at 3 and 7 d whereas the blue trace does not). Examination of $\Delta F/F_o$ plots suggested that whisker trimming only appeared to affect the amplitude of cortical responses to C1 whisker stimulation, but did not change the temporal kinetics of cortical responses (Fig. 2*A–C*). This is reflected in the fact that whisker trimming did not significantly alter the timing of peak sensory responses to C1 whisker deflection (Table 1) although there was a trend toward longer peak latencies in the 3 and 7 d trimmed groups. Similarly, the duration of cortical responses to C1 whisker deflection was not significantly affected by whisker trimming (Table 1).

Although VSD imaging is useful for visualizing whisker-evoked responses in multiple cortical areas, there tended to be variability in overall response amplitudes between each mouse.

Table 2. Summary of normalized peak C1 whisker responses ($\Delta F/F_o$) in each group and cortical region

	Control	3 d	7 d	21 d	One-way ANOVA
S1 cortex	1.10 ± 0.08	0.75 ± 0.08** ($t_{(13)} = 3.06, p < 0.005$)	0.72 ± 0.04** ($t_{(16)} = 4.28, p < 0.001$)	1.01 ± 0.03 ($t_{(12)} = 0.81, p = 0.21$)	$F_{(3,25)} = 9.19, p < 0.001$
S2 cortex	1.23 ± 0.08	0.93 ± 0.08* ($t_{(13)} = 2.44, p = 0.01$)	0.92 ± 0.09* ($t_{(15)} = 2.47, p = 0.01$)	1.16 ± 0.07 ($t_{(12)} = 0.61, p = 0.28$)	$F_{(3,25)} = 3.46, p = 0.03$
PA cortex	1.32 ± 0.12	0.83 ± 0.06** ($t_{(11)} = 2.86, p < 0.01$)	0.92 ± 0.12* ($t_{(14)} = 2.17, p = 0.02$)	1.21 ± 0.05 ($t_{(10)} = 0.63, p = 0.27$)	$F_{(3,21)} = 3.58, p = 0.03$

All data are expressed in means ± SE (*t* test and *p* values). All values in 3, 7, and 21 d compared to control values.
*$p < 0.05$, **$p < 0.01$.

However despite this variability between mice, we noticed that within in each trimmed mouse, C1 whisker responses were invariably lower than nondeprived whisker responses. Therefore to facilitate comparisons across mice, we normalized peak C1 whisker response amplitudes to the average peak response amplitudes of nondeprived whiskers A1, B1, D1, and E1 in each mouse. This was based on the fact that previous studies (Glazewski and Fox, 1996; Wilbrecht et al., 2010), as well as our own have shown that the amplitude of cortical responses to stimulation of nondeprived whiskers did not change significantly after trimming (compare blue traces in Fig. 2*A–C* across the different deprivation periods).

Examination of normalized C1 whisker responses (Fig. 2*D*) revealed a significant main effect of time after trimming on the peak amplitude of C1 whisker responses in S1 cortex ($F_{(3,25)} = 9.19$, $p = 0.0003$), S2 cortex ($F_{(3,25)} = 3.46$, $p = 0.03$) and PA cortex ($F_{(3,21)} = 3.58$, $p = 0.03$). Specifically, C1 whisker responses were significantly depressed in S1, S2, and PA cortical areas 3 and 7 d after C1 whisker trimming (Fig. 2*D*; also see Table 2 for statistical data). The depression of whisker responses in S1 cortex is consistent with previous studies using intrinsic signal optical imaging and electrophysiological recordings (Glazewski and Fox, 1996; Allen et al., 2003; Drew and Feldman, 2009). Consistent with previous studies (Brown and Dyck, 2002; Wimmer et al., 2010), this change was not permanent as whisker responses in all three cortical areas had returned to near control levels by 21 d when the C1 whisker had regrown (Fig. 2*D*, compare black and green bars). Thus, whisker trimming selectively depresses sensory responses to the trimmed whisker in primary, secondary and associative somatosensory cortical regions.

Trimming upregulates α4* nAChRs in the somatosensory cortex

Although cholinergic systems have long been implicated in higher order cognitive and sensory functions (Metherate, 2004), no studies to our knowledge have directly implicated nAChRs in experience-based depression of the somatosensory cortex. To test this idea, we used knock-in mice that express YFP on the α4* subunit of the nicotine receptor (Nashmi et al., 2007). Previous data has shown that inclusion of the YFP construct on the α4* subunit does not alter the normal expression of these receptors nor affect their function or sensitivity to agonists such as acetylcholine (Nashmi et al., 2007). Similar to VSD imaging experiments mentioned above, we trimmed C row whiskers on the left side of the face and then killed mice 3 h or 1, 3, 7, and 21 d after trimming. We then used confocal microscopy to image and quantify changes in the number of α4-YFP puncta in barrels from deprived row C and nondeprived rows B and D within layer 4 of the right S1 cortex (Fig. 3*A*,*B*). We focused on layer 4 because its vertical projections to layer 2/3 are a primary locus for experience-based cortical map plasticity (Allen et al., 2003).

To quantify changes in α4-YFP receptor expression across groups, we normalized α4-YFP puncta counts in row C to nondeprived rows within each mouse due to the fact that YFP signal (relative to background) varied from animal to animal due to slight differences in the level of tissue fixation. Our analysis revealed that trimming induced a progressive increase in the number of α4-YFP puncta within deprived row C barrels (Fig. 3*C*). The number of α4-YFP puncta was significantly increased 1, 3 and 7 d after trimming relative to control values (Fig. 3*C*, control = 0.95 ± 0.02 vs 1 d = 1.08 ± 0.02, $t_{(20)} = 3.04$, $p = 0.003$; vs 3 d = 1.18 ± 0.05, $t_{(19)} = 4.65$, $p < 0.001$; vs 7 d = 1.18 ± 0.05, $t_{(19)} = 4.49$, $p < 0.001$). Of note, the number of α4-YFP puncta at 3 h and 21 d after trimming when the whisker regrew, was not significantly different from controls (3 h = 0.94 ± 0.05, $t_{(17)} = 0.23$, $p = 0.4$; 21 d = 0.95 ± 0.07, $t_{(21)} = 0.01$, $p = 0.49$). In contrast with our analysis of puncta number, we found no effect of whisker trimming on the average size of each α4-YFP punctum in row C ($F_{(5,31)} = 0.26$, $p = 0.93$; control = 0.27 ± 0.01 μm^2, 3 h = 0.29 ± 0.01 μm^2, 1 d = 0.29 ± 0.01 μm^2, 3 d = 0.28 ± 0.005 μm^2, 7 d = 0.27 ± 0.03 μm^2, 21 d = 0.27 ± 0.02 μm^2). Collectively these results show that trimming increases the number of puncta associated with α4* nAChRs in deprived barrel columns in a manner that correlates spatially and temporally with the induction of functional cortical depression.

Since trimming whiskers upregulated the expression of α4* nAChRs, we then asked whether there might also be changes in the production of acetylcholine. Therefore, we unilaterally trimmed row C in three mice and quantified the expression of the acetylcholine-synthesizing enzyme, ChAT, in barrel cortex 3 d later. Our analysis indicated that trimming had no effect on the relative number of ChAT-stained puncta/fibers in deprived barrels (control row C = 1.04 ± 0.04 vs deprived row C = 1.00 ± 0.1, $t_{(3)} = 0.43$, $p = 0.35$).

Increased α4* nAChRs on GABAergic cortical neurons after trimming

How might an increase in the expression of α4* nAChRs in deprived barrel columns contribute to cortical depression? Currently there is no clear consensus on the cellular and subcellular distribution of these receptors, although electrophysiological and anatomical data suggest that nAChRs can modulate cortical excitability through either presynaptic or postsynaptic mechanisms (Lu et al., 1998; Alkondon et al., 2000; Christophe et al., 2002; Lambe et al., 2003; Oldford and Castro-Alamancos, 2003). To help address this question, we used an immunofluorescence approach and labeled brain sections from α4-YFP knock-in mice with neuron- and synapse-specific antibodies. Confocal imaging indicated that α4-YFP puncta primarily colocalized with neuronal cell bodies stained for NeuN (Fig. 4*A*), but sparse labeling in the neuropil was also detected. To further identify what types of neurons are targeted by α4* nAChRs, sections were immunola-

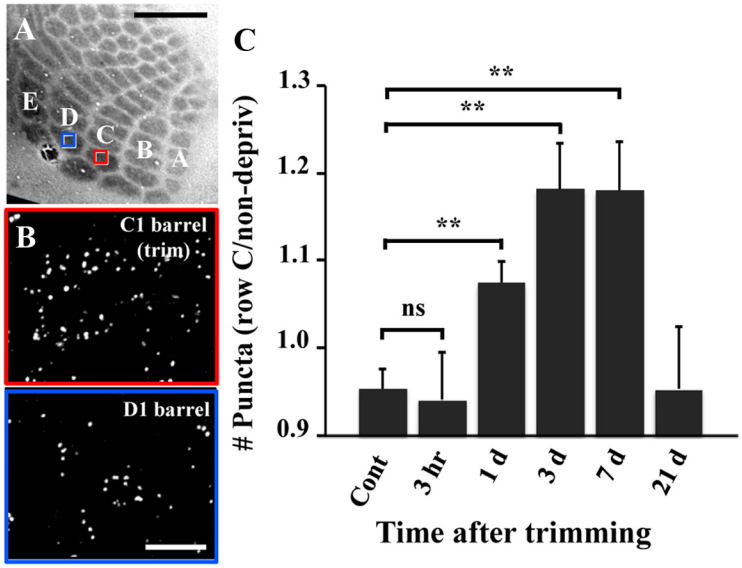

Figure 3. YFP-tagged α4* nAChRs are upregulated in somatosensory cortex after trimming. ***A***, Cytochrome oxidase-stained tangential section through layer 4 of the barrel cortex showing 5 rows of barrels (A–E) where the confocal images stacks of YFP-tagged α4* nAChRs were taken following trimming of row C whiskers. Scale bar, 500 μm. ***B***, Confocal images (maximum intensity *z* projection of 20 planar images) showing α4-YFP puncta in the deprived C1 barrel and nondeprived D1 barrel 7 d after trimming. On average, α4-YFP puncta were 0.37 ± 0.016 μm^2 in size. Scale bar, 10 μm. ***C***, Histogram showing relative changes in number of α4-YFP puncta in row C barrels versus nondeprived barrels. The number of α4-YFP puncta within each barrel was estimated in a standard volume of tissue (88,604 μm^3). α4-YFP puncta increased significantly in deprived barrels at 1, 3, and 7 d after trimming, but not at 3 h or 21 d when whiskers had regrown. $^{**}p < 0.005$, ns, Nonsignificant.

beled for the inhibitory amino acid GABA. α4-YFP puncta were expressed on the cell bodies of both GABA-positive and -negative cells. However, we should note that almost all GABA-positive cells in layer 4 (149 of 152 or 98%) had α4-YFP puncta decorating the soma (Fig. 4*B*). Considering that GABAergic neurons constitute ~20% of the total population of neurons in the somatosensory cortex, we could not be entirely sure from our previous experiment (Fig. 3) that trimming increased α4-YFP puncta on GABAergic neurons. Therefore, we unilaterally trimmed row C in mice (3 and 21 d survival) and quantified α4-YFP puncta on the cell bodies of GABA-positive and -negative neurons in layer 4. In control hemispheres (ipsilateral to trimming), there were typically more α4-YFP puncta on GABA-positive than -negative neurons in row C (GABA = 8.17 ± 0.30 vs non-GABA = 6.5 ± 0.44 puncta, $t_{(9)} = 3.01$, $p < 0.01$; Fig. 4*C*). Three days after trimming, we observed a significant increase in the number of α4-YFP puncta on GABAergic neurons in the deprived hemisphere relative to the undeprived control hemisphere (number of puncta on GABA neurons at 3 d = 9.4 ± 0.33 vs control = 8.17 ± 0.30, $t_{(7)} = 2.7$, $p < 0.05$, Fig. 4*C*). Twenty-one days after trimming when cortical depression subsides, the average number of α4-YFP puncta on GABAergic neurons decreased significantly in the deprived hemisphere relative to the 3 d trim group (number of puncta on GABA neurons at 21 d = 7.26 ± 0.25 vs 3 d = 9.4 ± 0.33, $t_{(8)} = 5.24$, $p < 0.01$; Fig. 4*C*) and was even below control hemisphere values ($t_{(9)} = 2.34$, $p < 0.05$).

To further understand the synaptic positioning of α4-YFP puncta, we examined whether YFP puncta colocalized with inhibitory, excitatory or cholinergic presynaptic terminals using antibodies for vesicular GABA, glutamate or acetylcholine transporters (VGAT, VGlut1,2, VAChT). Confocal imaging (Fig. 4*D*) showed that α4-YFP puncta rarely overlapped with VGAT (11 ± 1.6% colocalization), VGlut1 (6.6 ± 1.9% colocalization) or VGlut2 (10.6 ± 2.7% colocalization). VAChT-positive terminals often appeared to target neurons laden with α4-YFP. In some instances VAChT colocalized with α4-YFP puncta, but this was relatively infrequent (8.1 ± 1.6% colocalization, Fig. 4*D*). Colocalization with PSD-95 (Fig. 4*D*) was slightly higher but still relatively low (17.9 ± 3.2% colocalization). The fact that α4-YFP puncta did not typically colocalize with markers of excitatory, inhibitory or cholinergic terminals suggest that α4* nAChRs are likely positioned at perisynaptic or extrasynaptic sites.

Since previous studies have shown that some nAChRs are expressed on thalamocortical axons (Lambe et al., 2003; Disney et al., 2007), we labeled thalamic axons projecting to layer 4 of the barrel cortex using the anterograde tracer Mini-ruby (Fig. 4*E*). This experiment indicated relatively little colocalization between α4-YFP puncta and thalamic axons (Fig. 4*E*, 9.3 ± 0.9% colocalization).

Given the resolution limits of light microscopy, we could not be sure whether the α4-YFP labeling around cell bodies was in fact, expressed at the cell membrane, inside the cell body in intracellular organelles or perhaps in axon terminals that target the cell body. Therefore we performed immunoelectron microscopy on α4-YFP knock-in mice which coexpressed a HA epitope tag fused to α4 immediately upstream to the YFP tag. In accord with our fluorescence imaging data, bright-field microscopy indicated that HA reaction product had a punctate distribution that was found primarily around neuronal cell bodies (Fig. 5*A*). Consistent with previous electron microscopy studies (Nakayama et al., 1995; Arroyo-Jiménez et al., 1999; Commons, 2008), putative α4* nAChR expression was found in the endoplasmic reticulum, as well as near the plasma membrane of neuronal cell bodies and their apical dendrites (Fig. 5*B*,*C*, red arrows). Receptors expressed at the plasma membrane were often in the vicinity of unknown axon terminals with small clear vesicles, but were not typically associated with a postsynaptic density (Fig. 5*B*,*C*). In a few instances, α4* nAChRs located in the neuropil appeared to reside in putative presynaptic terminals (data not shown).

Activating α4* nAChRs *in vivo* mimics trimming-induced depression

Given that α4* nAChRs are expressed on the cell bodies of both inhibitory and excitatory neurons as well as some thalamocortical projections (Fig. 4), it is difficult to predict exactly what the functional consequences of activating this receptor will be *in vivo*. To link the increased expression of these receptors with cortical depression, we imaged whisker-evoked responses in control mice before, during and after topical application of the α4* nAChRs agonist RJR-2403 dissolved in aCSF. We chose this specific drug because unlike nicotine or acetylcholine, RJR-2403 is a potent and selective agonist for α4β2 nAChRs in the brain with lower affinity for other types of cholinergic receptors (Lippiello et al., 1996; Damaj et al., 1998, 1999). Within 5–10 min after topical application of 1 or 0.5 mM RJR-2403 to the cortex, peak S1 cortical responses to deflection of the C1 whisker were significantly reduced in magnitude by 40–50% (Fig. 6*A*,*B*; baseline = 0.16 ± 0.03 vs 5–10

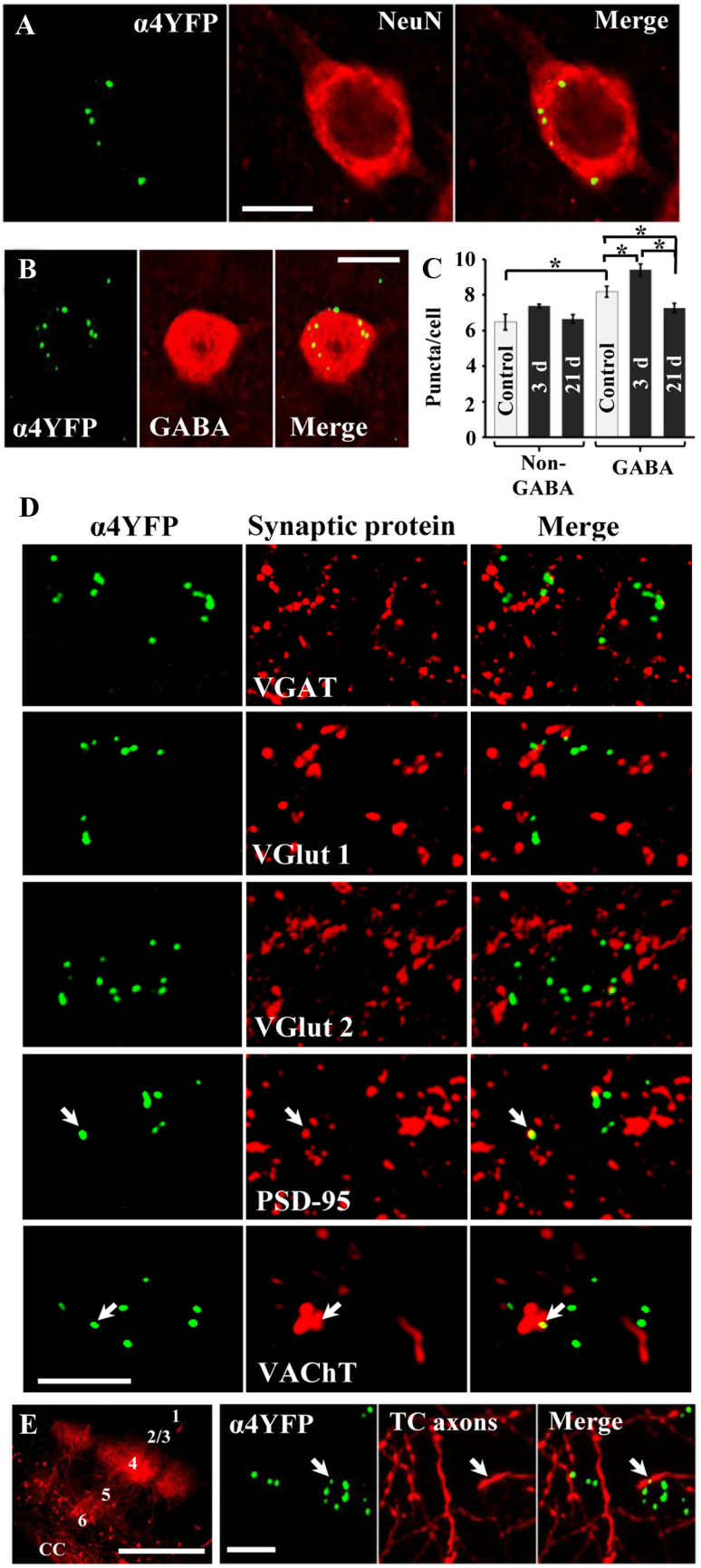

Figure 4. Trimming induces biphasic changes in the expression of $\alpha 4^*$ nAChRs on GABAergic cortical neurons. ***A***, ***B***, Single plane high-magnification confocal images (60× objective, NA = 1.3) showing α4-YFP puncta are associated with the neuron-specific protein NeuN and are highly expressed on GABA-stained cortical neurons. ***C***, Histogram showing average number of α4-YFP puncta on GABA-positive and -negative (non-GABA) cell bodies in mice 3 and 21 d after unilateral trimming of row C whiskers (dark bars). Note that the average number of α4-YFP puncta increases on GABAergic neurons 3 d after trimming and then decreases significantly by 21 d. Error bars represent SEM. $^*p < 0.05$. ***D***, Confocal images showing the distribution of α4-YFP puncta in relation to markers of inhibitory (VGAT), excitatory (VGlut1, 2) and cholinergic (VAChT) terminals, as well as PSD-95. α4-YFP puncta were often in close proximity to presynaptic markers but rarely showed direct overlap. α4-YFP puncta showed slightly greater colocalization with PSD-95 (see white arrows), although this was still relatively infrequent. ***E***, Thalamocortical (TC) axons innervating the barrel cortex were labeled with the anterograde tracer Mini-ruby. Scale bar, 500 μm. Analysis of α4-YFP puncta with Mini-ruby labeled axons in layer 4 revealed relatively little colocalization (9.3% of α4-YFP puncta colocalized with TC axons). Scale bars: ***A***, ***B***, ***D***, ***E***, 10 μm.

min = 0.08 ± 0.01, $t_{(12)} = 2.98$, $p = 0.006$; vs 10–15 min = 0.08 ± 0.01, $t_{(12)} = 2.76$, $p = 0.008$; vs 15–20 min = 0.10 ± 0.01, $t_{(12)} = 2.26$, $p = 0.02$). Both 0.5 and 1 mM agonist concentrations were equally effective in depressing S1 cortical responses ($t_{(5)} = 0.34$, $p = 0.37$). Similar to that observed in S1 cortex, sensory-evoked responses in S2 and PA cortex were reduced by 49 ± 7% and 41 ± 16%, respectively, within 5–10 min of agonist exposure. Furthermore, the depression of cortical responsiveness could be quickly reversed by washing out the drug with aCSF (Fig. 6*A*,*B*).

To refine the locus of these pharmacological effects, we micro-injected 0.5 mM RJR-2403 directly into the C1 barrel of layer 4 in the S1 cortex (Fig. 6*C*) while imaging whisker-evoked responses. As shown in Figure 6*D*, the amplitude of S1 cortical responses to C1 whisker deflection was significantly reduced after RJR-2403 injection (68 ± 9% decrease in amplitude relative to baseline amplitude, $t_{(2)} = 4.98$, $p = 0.02$; $n = 3$ mice). Conversely, microinjecting the $\alpha 4^*$ nAChR competitive antagonist DHβE into layer 4 of the barrel cortex transiently increased the amplitude of whisker-evoked responses (62 ± 13% increase relative to baseline amplitude, $t_{(2)} = 10.9$, $p = 0.004$, $n = 3$ mice), indicating that acetylcholine release is normally activating $\alpha 4^*$ nAChRs during whisker stimulation. Collectively, these findings show that activating $\alpha 4^*$ nAChRs *in vivo* can depress sensory evoked cortical responses in a manner similar to that seen 3–7 d after whisker trimming.

$\alpha 4^*$ nAChRs are required for the induction of cortical depression

If $\alpha 4^*$ nAChRs do in fact play a role in experience-based cortical depression, then chronically infusing an $\alpha 4^*$ nAChR

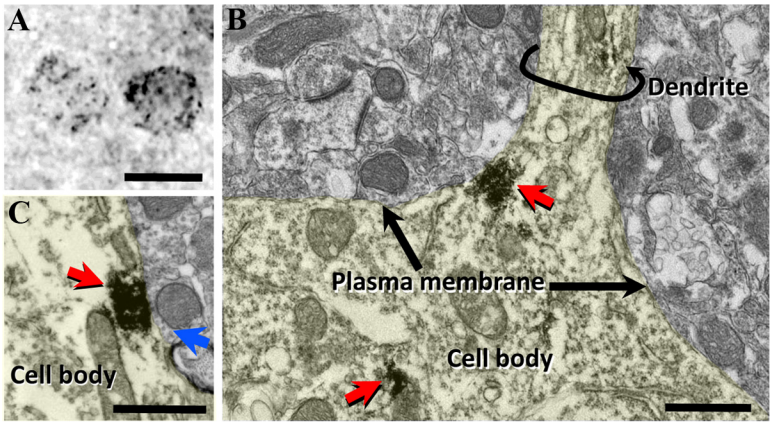

Figure 5. Subcellular distribution of α4* nAChRs in neurons. ***A***, Light micrograph of a brain section from a α4-YFP knock-in mice that was immunostained for HA. In these mice, the YFP-HA tag was inserted on the intracellular M3-M4 cytoplasmic loop of the α4 receptor. Control sections where HA antibody was omitted showed no detectable reaction product at the light microscopic level (data not shown). Scale bar, 10 μm. ***B***, Electron-dense reaction product (red arrows) was observed near the plasma membrane of cell bodies, as well as in the endoplasmic reticulum. ***C***, Electron micrograph showing putative α4* nAChR expression near the plasma membrane which is in proximity to a presynaptic terminal containing small vesicles (blue arrow). Scale bars: ***B***, ***C***, 1 μm.

antagonist in trimmed animals should prevent cortical depression *in vivo*. To test this idea, we trimmed the left C1 whisker and then subcutaneously implanted an osmotic mini-pump that was filled with the α4* nAChR antagonist DHβE (1 mg · kg h^{-1} over 3 d), or saline (Fig. 7*A*). A number of previous studies have shown that DHβE crosses the blood–brain barrier and can block the functional effects of α4* receptor activation *in vitro* and *in vivo* (Damaj et al., 1999; Jackson et al., 2009; Morishita et al., 2010). Mice infused with DHβE did not show any salient changes in ambulatory behavior, grooming or feeding. To ensure that DHβE was not still affecting cortical responses at the time of imaging, we recorded WEPs for 20–30 min before the DHβE injection (1 mg/kg, s.c.) and 120 min after the injection. These control experiments indicated that DHβE transiently increased the amplitude of cortical responses to whisker deflection that wore off within 120 min (Fig. 7*B*).

Three days after trimming, mini-pumps were removed (~3.5–5 h before the start of imaging) and mice were prepared for VSD imaging. As expected from our previous results (Figs. 1, 2), trimmed mice infused with saline showed robust depression of C1 whisker evoked responses in S1, S2, and PA cortex (Fig. 7*C*,*E*,*F*). By contrast, trimmed mice infused with DHβE showed little, if any depression of C1 whisker-evoked responses (Fig. 7*D*–*F*). It should be noted that DHβE treatment did not dampen general cortical responsiveness, given that response amplitudes in nondeprived whiskers were virtually identical for saline and DHβE-treated mice (Fig. 7*E*; peak $\Delta F/F_o$ for nondeprived whisker responses following saline or DHβE treatment is 0.196 ± 0.03 and 0.198 ± 0.05, respectively, $t_{(8)} = 0.03$, $p = 0.48$). Quantitative analysis of normalized response amplitudes (Fig. 7*F*) revealed little sign of cortical depression in DHβE-treated mice with a response profile similar to untrimmed control mice (untrimmed S1 response = 1.10 ± 0.07 vs DHβE = 1.01 ± 0.05, $t_{(12)} = 0.78$, $p = 0.22$; untrimmed S2 response = 1.23 ± 0.09 vs DHβE = 1.10 ± 0.12, $t_{(12)} = 1.01$, $p = 0.16$; untrimmed PA response = 1.32 ± 0.11 vs DHβE = 1.21 ± 0.12, $t_{(12)} = 0.55$, $p = 0.29$). In agreement with the finding that chronic DHβE prevented cortical depression, we found that DHβE infusion also prevented the trimming-related increase in α4-YFP puncta on GABAergic neurons in C row barrels (number of puncta/GABA neuron in trimmed mice receiving DHβE vs no drug = 8.25 ± 0.27 vs 9.40 ± 0.33, $t_{(7)} = 2.70$, $p = 0.01$, $n = 5$ mice). These results demonstrate that α4* nAChRs can regulate the induction of cortical depression *in vivo*.

Discussion

Mechanisms of experience-based cortical depression

Fluorescent signals derived from VSD imaging *in vivo* are composed primarily of postsynaptic membrane potentials from neurons located in superficial cortical layers (Ferezou et al., 2006; Berger et al., 2007). Using this approach, we show that 3–7 d of whisker disuse in fully mature mice leads to synaptic depression in multiple cortical regions associated with processing sensory information from the deprived whisker. We also found that trimming primarily reduced the peak amplitudes of trimmed whisker responses, but did not significantly affect the peak amplitude of cortical responses to stimulation of nondeprived whiskers. These results are in good agreement with electrophysiological investigations showing that depression is expressed in superficial cortical layers of the deprived barrel within 3–7 d of trimming and precedes cortical potentiation in nondeprived barrel columns (Glazewski and Fox, 1996; Allen et al., 2003; L. Li et al., 2009).

Experience-based cortical depression is thought to be mediated through long-term depression (LTD) like changes in the synaptic efficacy of layer 4 to layer 2/3 connections in deprived barrel columns (Fox, 1994; Allen et al., 2003; Wright et al., 2008). This raises the question of how might an increase in α4* nAChR expression in layer 4 lead to cortical depression? One clue from our data was that α4* nAChRs were highly expressed on GABAergic cortical interneurons and their relative levels of expression on these neurons increased following whisker trimming. This finding is consistent with previous work showing that mRNA for α4* nAChR are present in GABAergic cortical neurons (Porter et al., 1999; Couey et al., 2007). Furthermore, we show that activating α4* nAChRs *in vivo* by bath application or direct micro-injection of α4* nAChR agonist into layer 4 depressed whisker-evoked responses by 30–50% in control mice, similar to that seen after 3–7 d of whisker deprivation. Indeed, several electrophysiological studies using both human and rodent cortical tissue have shown that α4* nAChR activation rapidly depolarizes cortical interneurons, that can be blocked by the α4* nAChR antagonist DHβE (Xiang et al., 1998; Porter et al., 1999; Alkondon et al., 2000; Christophe et al., 2002; Klaassen et al., 2006; Couey et al., 2007; Mann and Mody, 2008). Therefore one possible mechanism underlying the depression of whisker-evoked responses is that α4* nAChRs may be enhancing GABAergic inhibition in deprived barrel columns. Whether this effect primarily involves inhibitory neurons in layer 4 or other cortical layers (layers 2/3 and 5) will require further investigation.

There have been several recent studies showing that certain GABAergic neurons in layer 4 are very sensitive to changes in whisker experience (Jiao et al., 2006; Lee et al., 2007; P. Li et al., 2009). However, the majority of these studies have suggested that there is a net reduction in GABAergic inhibition, as whisker trimming reduced the density of parvalbumin-positive inhibitory

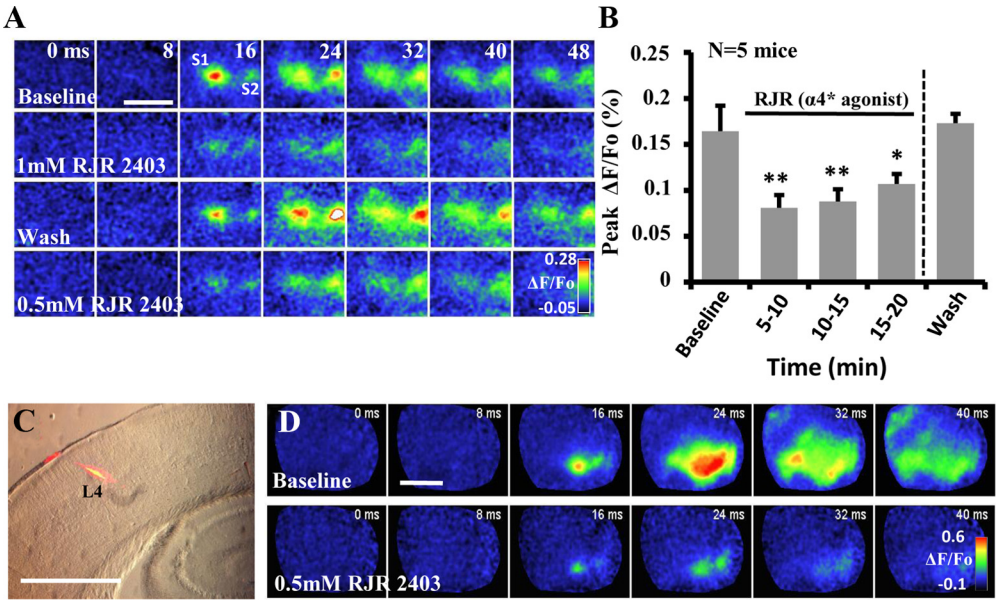

Figure 6. Activating α4* nAChRs *in vivo* depresses whisker-evoked cortical responses. ***A***, Voltage-sensitive dye imaging of C1 whisker-evoked cortical responses before (baseline) and after topical application of 1 or 0.5 mM of the neuronal α4* nAChR agonist RJR 2403 to the cortex of control mice. Each montage was generated from an average of 15 whisker stimulation trials which took ~5 min per trial to complete. Scale bar, 2 mm. ***B***, Histogram showing the average peak amplitudes of S1 cortex responses in 5 mice. Cortical depolarizations were significantly depressed 5–20 min after applying RJR 2403 to the cortex. Removing RJR 2403 and washing the brain with aCSF completely normalized cortical responses. Error bars represent SEM. ***C***, Coronal section showing the deposition 1% Texas Red dextran (red fluorescence) in experiments where RJR 2403 was micro-injected into layer 4 of the barrel cortex. Scale bar, 1 mm. ***D***, Montages showing whisker-evoked responses before (baseline) and after micro-injecting 0.5 mM RJR 2403 into barrel cortex. Scale bar, 2 mm. $*p < 0.05$, $**p < 0.01$.

neurons and their perisomatic inhibitory boutons in layer 4 (Jiao et al., 2006). Further, whole-cell recordings of action potential firing properties and ion channel conductances in these cells indicated a net reduction in their intrinsic excitability (Sun, 2009). This raises the question of how might the present data fit with past studies. One important thing to consider is that past studies repeatedly trimmed whiskers in neonatal animals for several weeks. It is possible that repeated trimming, unlike a single bout of trimming, may induce a homeostatic-like reduction in inhibitory neuron function to compensate for the chronic reduction in afferent sensory driven neuronal activity (Sun, 2009). Second, since inhibitory connectivity and $GABA_A$ receptor signaling (based on changes in the chloride concentration gradient) are still developing in the first month of postnatal development, sensory deprivation may have very different effects on inhibitory circuits depending on what age deprivation was initiated. Indeed Maffei et al. (2010) showed that monocular deprivation can depress inhibitory synapses in visual cortex when initiated in the third postnatal week, but potentiate these synapses if monocular deprivation is started in the fourth postnatal week. Whether GABAergic inhibition is strengthened in adult barrel cortex in the first couple days after trimming has not been examined, although a recent report in visual cortex demonstrated that inhibitory neurons show a bias in spiking toward deprived eye columns following acute sensory deprivation which reverses in polarity after long-term deprivation (Yazaki-Sugiyama et al., 2009). Further, a recent slice imaging study showed that 3 d of monocular deprivation specifically reduced layer 4 output to layer 2/3 that was accompanied by enhanced inhibition within layer 4 (Wang et al., 2011). Nonetheless, future studies will be required to unravel how α4* nAChRs modulate inhibitory neuron function in layer 4 or in other cortical layers (i.e., layers 2/3 and 5), especially in the acute stages of whisker deprivation.

Subcellular distribution of α4* nAChRs in somatosensory cortex

It is well established that nAChR-mediated neurotransmission can modulate cortical excitability. Previous studies have shown that micro-injection or bath application of nicotine can increase the excitability of corticothalamic (Kassam et al., 2008), entorhinal (Tu et al., 2009) and prefrontal cortical neurons (Vidal and Changeux, 1993; Lambe et al., 2003). However as noted previously, nicotine can also depolarize inhibitory cortical neurons (Couey et al., 2007). Therefore, there is increasing recognition that the effect of nicotine on cortical excitability is complex and depends largely on what specific type of neuron (pyramidal vs interneuron) or nAChR subtype is activated (e.g., α4, α7 subunits) and what region of cortex is examined (Metherate, 2004). To understand the subcellular distribution of α4* nAChRs in layer 4 of primary somatosensory cortex, we used both confocal and electron microscopy. Immunofluorescent staining for various cell and synapse-specific proteins revealed that α4-YFP puncta rarely colocalized with markers of presynaptic glutamate and GABAergic axon terminals. Furthermore, our thalamic and VGlut2 labeling experiments indicated that only a small fraction of α4-YFP puncta colocalized with thalamocortical axons in layer 4 of the barrel cortex. Although this observation may not be generalized to other brain regions such as prefrontal cortex (Vidal and Changeux, 1993; Lambe et al., 2003), we should note that the relatively scant colocalization of α4* nAChRs with presynaptic structures in the present work is consistent with ultrastructural examination of these receptors in rat somatosensory cortex and dorsal raphe nucleus (Nakayama et al., 1995; Commons, 2008). Our ultrastructural analysis indicated that α4* nAChRs were often associated with peri- or extrasynaptic sites on neuronal cell bodies. This finding is supported by electron microscopy studies showing that α4* nAChRs are detected near the

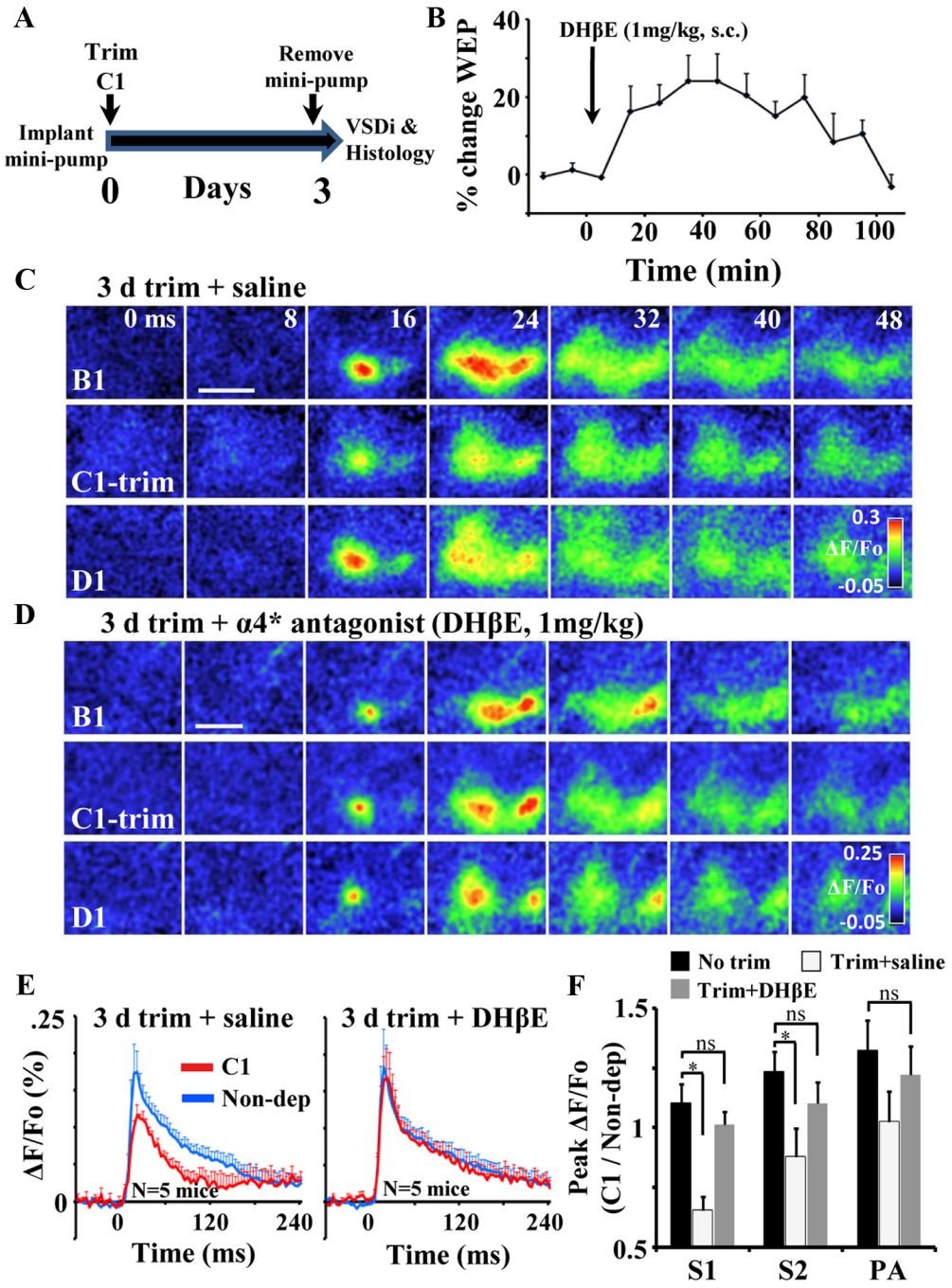

Figure 7. Cortical depression can be prevented by chronic infusion of α4* nAChR antagonist DHβE. ***A***, Summary of experiments used to determine whether α4* nAChRs are required for cortical depression. Adult mice had the left C row whiskers trimmed and then were implanted with osmotic mini-pumps to infuse either saline or DHβE for 3 d. On the third day, mini-pumps were removed and mice were either imaged or processed for histological analysis of α4-YFP puncta. ***B***, Recording of WEPs in barrel cortex indicated that the effects of subcutaneous injection of DHβE (1 mg/kg) on cortical responses lasted ~90–120 min and had worn off by the time of VSD imaging (which started >3.5 h after mini-pump removal on day 3). ***C***, Montage shows clear depression of C1 whisker-evoked cortical responses in trimmed mice chronically infused with saline. Each montage represents an average of 15 stimulation trials per whisker. ***D***, Mice chronically infused with DHβE do not show trimming-induced cortical depression. ***E***, Plots show average percentage changes in fluorescence in S1 cortex following stimulation of deprived C1 (red trace) or nondeprived whiskers (blue traces) in saline- or DHβE-treated mice. ***F***, Normalized peak cortical responses show that, unlike trimmed mice infused with saline (white bars), trimmed mice given DHβE (gray bar) do not show depression of C1 responses in S1, S2, and PA cortex. Further, peak response amplitudes to the C1 whisker in mice administered DHβE were not significantly different from untrimmed control mice (black bar). Error bars represent SEM. *$p < 0.05$. Scale bars: ***C***, ***D***, 2 mm.

plasma membrane of neuronal cell bodies and apical dendritic shafts, but not typically at postsynaptic densities (Nakayama et al., 1995; Commons, 2008). Whether α4* nAChR are directly apposed by cholinergic terminals is not entirely clear, however our immunofluorescence data suggest a loose spatial relationship between α4* nAChRs and cholinergic terminals, similar to that described for α7 nAChRs and muscarinic receptors (Jones and Wonnacott, 2004; Yamasaki et al., 2010).

In conclusion, we show that whisker trimming in adult mice leads to depression of whisker-evoked cortical responses. Depression of cortical responses was associated with an increase in α4* nAChRs in layer 4 of the deprived barrel column. Confo-

cal and electron microscopic analysis revealed that α4* nAChRs in layer 4 were preferentially expressed on neuronal cell bodies, especially GABAergic interneurons. Therefore one possible mechanism for cortical depression could be related to α4* nAChRs enhancing inhibition in the deprived barrel column. Indeed, we found that pharmacologically activating α4* nAChRs could depress sensory-evoked responses in normal mice, whereas blocking these receptors prevented trimming-induced depression *in vivo*. However, given that α4* nAChRs are also expressed on excitatory neurons and some thalamic axons, future studies will be needed to directly determine whether depression occurs through enhanced activation of GABAergic neurons or through weakened excitatory neurotransmission of thalamocortical or intracortical pathways.

References

Alkondon M, Pereira EF, Eisenberg HM, Albuquerque EX (2000) Nicotinic receptor activation in human cerebral cortical interneurons: a mechanism for inhibition and disinhibition of neuronal networks. J Neurosci 20:66–75.

Allen CB, Celikel T, Feldman DE (2003) Long-term depression-induced by sensory deprivation during cortical map plasticity in vivo. Nat Neurosci 6:291–299.

Arroyo-Jiménez MM, Bourgeois JP, Marubio LM, Le Sourd AM, Ottersen OP, Rinvik E, Fairén A, Changeux JP (1999) Ultrastructural localization of the alpha4-subunit of the neuronal acetylcholine nicotinic receptor in the rat substantia nigra. J Neurosci 19:6475–6487.

Barik J, Wonnacott S (2009) Molecular and cellular mechanisms of action of nicotine in the CNS. Handb Exp Pharmacol 2009:173–207.

Benison AM, Ard TD, Crosby AM, Barth DS (2006) Temporal patterns of field potentials in vibrissa/barrel cortex reveal stimulus orientation and shape. J Neurophysiol 95:2242–2251.

Berger T, Borgdorff A, Crochet S, Neubauer FB, Lefort S, Fauvet B, Ferezou I, Carleton A, Lüscher HR, Petersen CC (2007) Combined voltage and calcium epifluorescence imaging in vitro and in vivo reveals subthreshold and suprathreshold dynamics of mouse barrel cortex. J Neurophysiol 97:3751–3762.

Brett-Green B, Paulsen M, Staba RJ, Fifková E, Barth DS (2004) Two distinct regions of secondary somatosensory cortex in the rat: topographical organization and multisensory responses. J Neurophysiol 91:1327–1336.

Brown CE, Dyck RH (2002) Rapid, experience-dependent changes in levels of synaptic zinc in primary somatosensory cortex of the adult mouse. J Neurosci 22:2617–2625.

Brown CE, Aminoltejari K, Erb H, Winship IR, Murphy TH (2009) *In vivo* voltage-sensitive dye imaging in adult mice reveals that somatosensory maps lost to stroke are replaced over weeks by new structural and functional circuits with prolonged modes of activation within both the peri-infarct zone and distant sites. J Neurosci 29:1719–1734.

Buonomano DV, Merzenich MM (1998) Cortical plasticity: from synapses to maps. Annu Rev Neurosci 21:149–186.

Changeux JP (2010) Nicotine addiction and nicotinic receptors: lessons from genetically modified mice. Nat Rev Neurosci 11:389–401.

Christophe E, Roebuck A, Staiger JF, Lavery DJ, Charpak S, Audinat E (2002) Two types of nicotinic receptors mediate an excitation of neocortical layer I interneurons. J Neurophysiol 88:1318–1327.

Clem RL, Celikel T, Barth AL (2008) Ongoing in vivo experience triggers synaptic metaplasticity in the neocortex. Science 319:101–104.

Commons KG (2008) Alpha4 containing nicotinic receptors are positioned to mediate postsynaptic effects on 5-HT neurons in the rat dorsal raphe nucleus. Neuroscience 153:851–859.

Conner JM, Culberson A, Packowski C, Chiba AA, Tuszynski MH (2003) Lesions of the Basal forebrain cholinergic system impair task acquisition and abolish cortical plasticity associated with motor skill learning. Neuron 38:819–829.

Conner JM, Chiba AA, Tuszynski MH (2005) The basal forebrain cholinergic system is essential for cortical plasticity and functional recovery following brain injury. Neuron 46:173–179.

Couey JJ, Meredith RM, Spijker S, Poorthuis RB, Smit AB, Brussaard AB, Mansvelder HD (2007) Distributed network actions by nicotine increase the threshold for spike-timing-dependent plasticity in prefrontal cortex. Neuron 54:73–87.

Dachtler J, Hardingham NR, Glazewski S, Wright NF, Blain EJ, Fox K (2011) Experience-dependent plasticity acts via GluR1 and a novel neuronal nitric oxide synthase-dependent synaptic mechanism in adult cortex. J Neurosci 31:11220–11230.

Damaj MI, Fei-Yin M, Dukat M, Glassco W, Glennon RA, Martin BR (1998) Antinociceptive responses to nicotinic acetylcholine receptor ligands after systemic and intrathecal administration in mice. J Pharmacol Exp Ther 284:1058–1065.

Damaj MI, Glassco W, Aceto MD, Martin BR (1999) Antinociceptive and pharmacological effects of metanicotine, a selective nicotinic agonist. J Pharmacol Exp Ther 291:390–398.

Dani JA (2001) Overview of nicotinic receptors and their roles in the central nervous system. Biol Psychiatry 49:166–174.

Disney AA, Aoki C, Hawken MJ (2007) Gain modulation by nicotine in macaque v1. Neuron 56:701–713.

Drew PJ, Feldman DE (2009) Intrinsic signal imaging of deprivation-induced contraction of whisker representations in rat somatosensory cortex. Cereb Cortex 19:331–348.

Ferezou I, Bolea S, Petersen CC (2006) Visualizing the cortical representation of whisker touch: voltage-sensitive dye imaging in freely moving mice. Neuron 50:617–629.

Ferezou I, Haiss F, Gentet LJ, Aronoff R, Weber B, Petersen CC (2007) Spatiotemporal dynamics of cortical sensorimotor integration in behaving mice. Neuron 56:907–923.

Fox K (1994) The cortical component of experience-dependent synaptic plasticity in the rat barrel cortex. J Neurosci 14:7665–7679.

Frostig RD, Xiong Y, Chen-Bee CH, Kvasnák E, Stehberg J (2008) Large-scale organization of rat sensorimotor cortex based on a motif of large activation spreads. J Neurosci 28:13274–13284.

Glazewski S, Fox K (1996) Time course of experience-dependent synaptic potentiation and depression in barrel cortex of adolescent rats. J Neurophysiol 75:1714–1729.

Grinvald A, Hildesheim R (2004) VSDI: a new era in functional imaging of cortical dynamics. Nat Rev Neurosci 5:874–885.

Jackson KJ, Kota DH, Martin BR, Damaj MI (2009) The role of various nicotinic receptor subunits and factors influencing nicotine conditioned place aversion. Neuropharmacology 56:970–974.

Jiao Y, Zhang C, Yanagawa Y, Sun QQ (2006) Major effects of sensory experiences on the neocortical inhibitory circuits. J Neurosci 26:8691–8701.

Jones IW, Wonnacott S (2004) Precise localization of alpha7 nicotinic acetylcholine receptors on glutamatergic axon terminals in the rat ventral tegmental area. J Neurosci 24:11244–11252.

Juliano SL, Ma W, Eslin D (1991) Cholinergic depletion prevents expansion of topographic maps in somatosensory cortex. Proc Natl Acad Sci U S A 88:780–784.

Kassam SM, Herman PM, Goodfellow NM, Alves NC, Lambe EK (2008) Developmental excitation of corticothalamic neurons by nicotinic acetylcholine receptors. J Neurosci 28:8756–8764.

Kilgard MP, Merzenich MM (1998) Cortical map reorganization enabled by nucleus basalis activity. Science 279:1714–1718.

Klaassen A, Glykys J, Maguire J, Labarca C, Mody I, Boulter J (2006) Seizures and enhanced cortical GABAergic inhibition in two mouse models of human autosomal dominant nocturnal frontal lobe epilepsy. Proc Natl Acad Sci U S A 103:19152–19157.

Lambe EK, Picciotto MR, Aghajanian GK (2003) Nicotine induces glutamate release from thalamocortical terminals in prefrontal cortex. Neuropsychopharmacology 28:216–225.

Lee SH, Land PW, Simons DJ (2007) Layer- and cell-type-specific effects of neonatal whisker-trimming in adult rat barrel cortex. J Neurophysiol 97:4380–4385.

Li L, Bender KJ, Drew PJ, Jadhav SP, Sylwestrak E, Feldman DE (2009) Endocannabinoid signaling is required for development and critical period plasticity of the whisker map in somatosensory cortex. Neuron 64:537–549.

Li P, Rudolph U, Huntsman MM (2009) Long-term sensory deprivation selectively rearranges functional inhibitory circuits in mouse barrel cortex. Proc Natl Acad Sci U S A 106:12156–12161.

Lippiello PM, Bencherif M, Gray JA, Peters S, Grigoryan G, Hodges H, Collins AC (1996) RJR-2403: a nicotinic agonist with CNS selectivity II. In vivo characterization. J Pharmacol Exp Ther 279:1422–1429.

Lu Y, Grady S, Marks MJ, Picciotto M, Changeux JP, Collins AC (1998) Pharmacological characterization of nicotinic receptor-stimulated GABA release from mouse brain synaptosomes. J Pharmacol Exp Ther 287:648–657.

Maalouf M, Miasnikov AA, Dykes RW (1998) Blockade of cholinergic receptors in rat barrel cortex prevents long-term changes in the-evoked potential during sensory preconditioning. J Neurophysiol 80:529–545.

Maffei A, Lambo ME, Turrigiano GG (2010) Critical period for inhibitory plasticity in rodent binocular V1. J Neurosci 30:3304–3309.

Mann EO, Mody I (2008) The multifaceted role of inhibition in epilepsy: seizure-genesis through excessive GABAergic inhibition in autosomal dominant nocturnal frontal lobe epilepsy. Curr Opin Neurol 21:155–160.

McKay BE, Placzek AN, Dani JA (2007) Regulation of synaptic transmission and plasticity by neuronal nicotinic acetylcholine receptors. Biochem Pharmacol 74:1120–1133.

Metherate R (2004) Nicotinic acetylcholine receptors in sensory cortex. Learn Mem 11:50–59.

Morishita H, Miwa JM, Heintz N, Hensch TK (2010) Lynx1, a cholinergic brake, limits plasticity in adult visual cortex. Science 330:1238–1240.

Nakayama H, Shioda S, Okuda H, Nakashima T, Nakai Y (1995) Immunocytochemical localization of nicotinic acetylcholine receptor in rat cerebral cortex. Brain Res Mol Brain Res 32:321–328.

Nashmi R, Xiao C, Deshpande P, McKinney S, Grady SR, Whiteaker P, Huang Q, McClure-Begley T, Lindstrom JM, Labarca C, Collins AC, Marks MJ, Lester HA (2007) Chronic nicotine cell specifically upregulates functional alpha 4* nicotinic receptors: basis for both tolerance in midbrain and enhanced long-term potentiation in perforant path. J Neurosci 27:8202–8218.

Oldford E, Castro-Alamancos MA (2003) Input-specific effects of acetylcholine on sensory and intracortical-evoked responses in the "barrel cortex" in vivo. Neuroscience 117:769–778.

Petersen CC, Grinvald A, Sakmann B (2003) Spatiotemporal dynamics of sensory responses in layer 2/3 of rat barrel cortex measured *in vivo* by voltage-sensitive dye imaging combined with whole-cell voltage recordings and neuron reconstructions. J Neurosci 23:1298–1309.

Porter JT, Cauli B, Tsuzuki K, Lambolez B, Rossier J, Audinat E (1999) Selective excitation of subtypes of neocortical interneurons by nicotinic receptors. J Neurosci 19:5228–5235.

Prusky GT, Shaw C, Cynader MS (1988) The distribution and ontogenesis of [^{3}H]nicotine binding sites in cat visual cortex. Brain Res 467:161–176.

Rema V, Armstrong-James M, Ebner FF (1998) Experience-dependent plasticity of adult rat S1 cortex requires local NMDA receptor activation. J Neurosci 18:10196–10206.

Shulz DE, Sosnik R, Ego V, Haidarliu S, Ahissar E (2000) A neuronal analogue of state-dependent learning. Nature 403:549–553.

Sun QQ (2009) Experience-dependent intrinsic plasticity in interneurons of barrel cortex layer IV. J Neurophysiol 102:2955–2973.

Takahashi T, Svoboda K, Malinow R (2003) Experience strengthening transmission by driving AMPA receptors into synapses. Science 299:1585–1588.

Tu B, Gu Z, Shen JX, Lamb PW, Yakel JL (2009) Characterization of a nicotine-sensitive neuronal population in rat entorhinal cortex. J Neurosci 29:10436–10448.

Vidal C, Changeux JP (1993) Nicotinic and muscarinic modulations of excitatory synaptic transmission in the rat prefrontal cortex in vitro. Neuroscience 56:23–32.

Wallace DJ, Sakmann B (2008) Plasticity of representational maps in somatosensory cortex observed by in vivo voltage-sensitive dye imaging. Cereb Cortex 18:1361–1373.

Wallace H, Fox K (1999) Local cortical interactions determine the form of cortical plasticity. J Neurobiol 41:58–63.

Wang L, Fontanini A, Maffei A (2011) Visual experience modulates spatiotemporal dynamics of circuit activation. Front Cell Neurosci 5:12.

Wiesel TN, Hubel DH (1963) Single-cell responses in striate cortex of kittens deprived of vision in one eye. J Neurophysiol 26:1003–1017.

Wilbrecht L, Holtmaat A, Wright N, Fox K, Svoboda K (2010) Structural plasticity underlies experience-dependent functional plasticity of cortical circuits. J Neurosci 30:4927–4932.

Wimmer VC, Broser PJ, Kuner T, Bruno RM (2010) Experience-induced plasticity of thalamocortical axons in both juveniles and adults. J Comp Neurol 518:4629–4648.

Wright N, Glazewski S, Hardingham N, Phillips K, Pervolaraki E, Fox K (2008) Laminar analysis of the role of GluR1 in experience-dependent and synaptic depression in barrel cortex. Nat Neurosci 11:1140–1142.

Xiang Z, Huguenard JR, Prince DA (1998) Cholinergic switching within neocortical inhibitory networks. Science 281:985–988.

Yamasaki M, Matsui M, Watanabe M (2010) Preferential localization of muscarinic M1 receptor on dendritic shaft and spine of cortical pyramidal cells and its anatomical evidence for volume transmission. J Neurosci 30:4408–4418.

Yazaki-Sugiyama Y, Kang S, Câteau H, Fukai T, Hensch TK (2009) Bidirectional plasticity in fast-spiking GABA circuits by visual experience. Nature 462:218–221.